

FORMATION DAMAGE IN THE INTER-WELL ZONES: EXPERIMENTS AND ADVANCED ANALYTICS

Denis Orlov, Dmitry Koroteev

Skolkovo Institute of Science and Technology, Skolkovo Innovation Center, Building 3,
Moscow, 143026, Russia

This paper was prepared for presentation at the International Symposium of the Society of Core Analysts held in Trondheim, Norway, 27-30 August 2018

ABSTRACT

We present a predictive model of formation damage in Vendian deposits based on the analysis of rock properties and flooding conditions. We have studied all the features of the self-colmatation process and arrange them in accordance with their importance. We have used two approaches to obtain the results. The first one was to discover all possible 2D cross-plot correlations between colmatation characteristics and features (manual analysis). The second is based on machine learning algorithms. The benefits and disadvantages of both approaches were discussed in details.

INTRODUCTION

The unpredictable decline in productivity and injectivity of wells due to formation damage or colmatation is an important problem of petroleum engineering [1, 2]. The origin of the formation damage mechanisms varies from fines migration and retention to adsorption processes. Moreover, the mechanism of colmatation is dependant on an area of interest: near-well or inter-well zone. In some cases, the colmatation happens not only in the near wellbore zone but cover a significant part of a reservoir.

The focus of our research is on fines migration in porous media in the case when influent fluid is free of any solid particles. Only the fine particles that are naturally present in porous media of a reservoir rock (in-situ particles) and can be released and entrained with the flowing fluid are considered. These entrained particles can be trapped in pores and cause a significant permeability reduction [1]. This type of formation damage (self-colmatation) is commonly related to flows in inter-well area of reservoir.

The key objective of this work was to investigate colmatation in more complex reservoir rocks than it has been considered before. Our objects were sandstones of the Lower Vendian deposits of the Nepa-Botuoba Arch, which is the second largest dome-shaped regional high of Eastern Siberia. Water filtration in these reservoir rocks has a strong self-colmatation feature: entrainment of the in-situ fines during injection of initially clean water to core samples [3].

PROBLEM STATEMENT AND APPLIED METHODS

Our previous study [3] showed that natural cores from Vendian deposits demonstrate self-colmatation during water filtration even with relatively high (3%) constant salinity which was a sufficient extension of observations from [4]. Corresponding permeability

reduction was registered in cores with a wide range of porosity, absolute permeability and residual oil saturation. We also performed some tests with a single-phase oil filtration. The permeability decrease was observed only when water is flowing in the porous space. And there were no colmatation in the case of oil-flooding. Water itself was shown to be a strong driver of self-colmatation, which is likely because of its intensive physicochemical reaction with pore surface.

Experimental procedure is described in [3]. The self-colmatation at single-phase water flooding was studied during 22 lab tests. Each core model was composed of two or three samples with the similar porosity, permeability, mineral composition and granulometric distribution. Experiments conditions are presented in Table 1.

Table 1. Conditions of the experiments

N ₂	Condition	Value	N ₂	Condition	Value
1	model of oil	N-decane (C ₁₀ H ₁₂)	6	pressure drop accuracy	0.5%
2	Initial saturation	residual oil saturation	7	saturation accuracy	10%
3	confining pressure	50 MPa	8	NaCl concentration	30 g/l
4	pore pressure	12 MPa	9	Water viscosity	1 cP
5	temperature	Ambient (23C)	10	Water density	1.02 g/cc

In addition to water flooding experiments, some of the core samples were tested to estimate a grain size distribution, mineral composition with X-ray diffraction and pore throat distribution with semipermeable membrane method for capillary pressure measurement.

Core samples characteristics we used in the experiments are in Figure 1. One can spot a significant variation in porosity ($m=6-21\%$), absolute permeability ($K=10-1650$ mD) and the residual oil saturation ($S_{or}=30-70\%$).

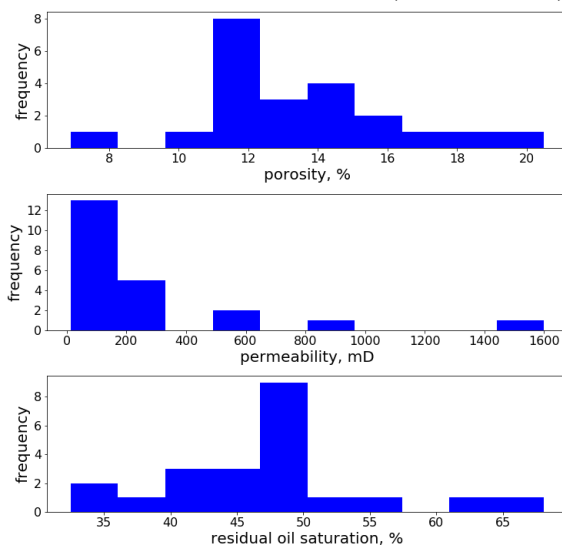


Figure. 1. Distributions of core parameters.

The core features do not follow a normal (Gaussian) form of distribution. It is especially noticeable for permeability data. This reduces the potential of applications of some of classical machine learning techniques. Moreover, because of the complex structure of productive intervals of Vendian deposits, these core samples do not have strong K-m correlations. All these constraints of dataset increase uncertainties of colmatation prediction and analysis.

All water-flooding experiments were performed at residual oil saturations. Development of colmatation was characterized by the growth of differential pressure after water breakthrough. After injection of 3.5-20 pore volumes of water, the total permeability was reduced by a factor of 1.02 to 4.76.

Previous research showed that the pressure drop dynamics demonstrates five typical patterns (Figure 2). The purpose of the classification was to define a simple criterion for evaluating the mechanism driving retention and correlate it with some of rock properties and flooding conditions. Type I corresponds to the classical no-colmatation regime of filtration, when pressure drop over the core model decrease monotonically with water injection ($\Delta P(t)/\Delta P_0 < 1$, $\Delta P(t)$ – pressure drop in time, ΔP_0 – initial pressure drop). Types II and III presents two boundary cases: unlimited and limited formation damage respectively ($\Delta P(t)/\Delta P_0 \geq 1$). Unlimited (Type II) formation damage refers to the monotonic rise of $\Delta P(t)$ with increasing growth rates throughout the duration of the constant-rate filtration process. Type III corresponds to decreasing permeability to a new steady level with a stabilized pressure drop at some flow rate. This classification will be further used in determination of correlations between colmatation and rock properties. It will be shown that within each type we can find more tight correlations.

Colmatation is a non-steady behavior of a flooding system with a time-dependent normalized permeability $K(t)/K_0$. Thus, to estimate correlations between colmatation, rock properties, and flooding conditions one should find one or more unique colmatation characteristics which are able to describe the dynamic of permeability reduction. We found it more sensible to present $K(t)/K_0$ as a function of injected water pore volumes (V_{inj}) and study the function's parameters dependencies on rock properties and experimental conditions.

There is a widely used approximation representing the normalized permeability K/K_0 as an inverse function of the retained fine concentration (σ) [5, 6]:

$$\frac{K(\sigma)}{K_0} = \frac{1}{1 + \beta\sigma}, \quad (1)$$

where β is the formation damage coefficient. If β is large, even a small retained concentration causes an intensive permeability reduction. σ in eq. (1) can be considered as the concentration of plugged fines. Knowing fines concentration in the inlet and the outlet flow, it is possible to count σ in each time moment and predict permeability reduction at a specific value of β . Unfortunately, at self-colmatation, we do not have enough information about in-situ fines concentrations. To solve this problem, we used a method from [7], which contains an assumption that σ can be related to the amount of the water (V) that passed through the area of a porous sample denoted as A :

$$\frac{k/k_0 - R_{min}}{1 - R_{min}} = \frac{1}{(1 + \alpha(V/A)^n)}, \quad (2)$$

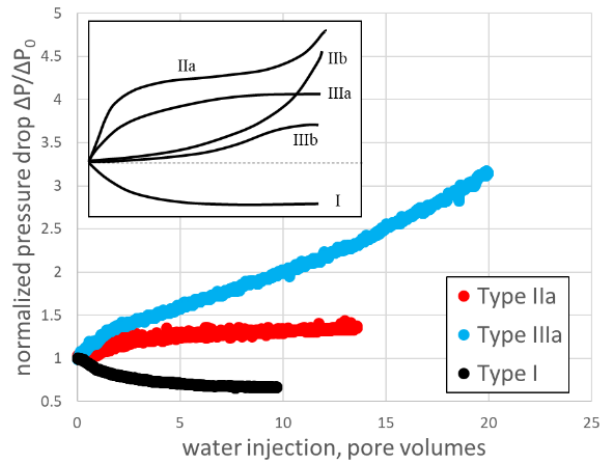


Figure 2. Different types of colmatation.

where α , n , and R_{min} are the three governing parameters of the model. α represents the intensity of the damage. n defines the shape of the damage curve. R_{min} sets an asymptotic limit for permeability reduction ($k_{min}=k_0 * R_{min}$).

We have used equation 2 as basic approximation to investigate correlations between α , n , R_{min} and rock properties together with flooding conditions. Results of the best approximation for each experiment are presented in [3] and the frequency distributions of α , n , and R_{min} are in Figure 3.

COLMATATION PREDICTION RESULTS

Described approach allows defining dependences of all three governing parameters (α , n , and R_{min}) on different features of the experiments. We used 16 features for further analysis: porosity m , absolute permeability K_{abs} , pore volume V_{por} , initial oil saturation S_{or} , pressure drop type, 3 characteristics of pore throat size distribution, 3 characteristics of grain size distribution, 4 characteristics of mineral content distribution, and horizon (Talakh, Khamakin or Botuobinsk). The characteristics of pore throat size distribution were fractions of pore throats with sizes $d_p = 6-12 \mu\text{m}$, $d_p = 12-30 \mu\text{m}$, and $d_p > 30 \mu\text{m}$. And the characteristics of grain size distribution were fractions of grains with sizes $d_g = 0.05-0.01 \text{ mm}$, $d_g = 0.1-0.25 \text{ mm}$, and $d_g = 0.25-0.5 \text{ mm}$. Contents of microcline, dolomite, anhydrite, and quartz were used as 4 characteristics of mineral concentration distribution.

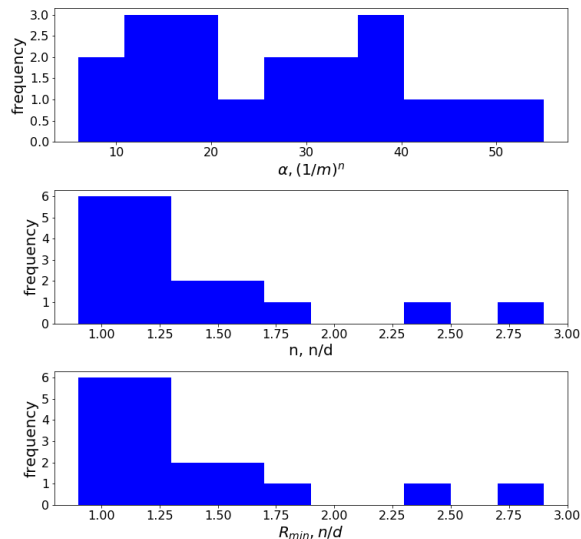


Figure 3. Distributions of colmatation parameters.

For the first step we have tried to find correlations between each of α , n , and R_{min} and each of 16 features independently (using the cross-plot charts). Unfortunately, it was not possible to find any correlations within horizon types because of a small dataset and non-Gaussian distribution of features in each type. We could not find the correlations between α , n , R_{min} and porosity and pore volume: the coefficient of determination R^2 was negative in both cases. All analytical data concerning influence of any of 13 residual features on colmatation intensity is presented in Table 2. We have estimated R^2 for Type II and Type

III separately. And within each type it has been obtained a more tight correlations with higher value of R^2 .

The intensity of the formation damage α and the exponent n are increasing and the factor R_{min} is decreasing with the colmatation amplification. We assume weak correlation between colmatation parameters and a feature of consideration if we have a mismatch in any trend direction (if the trend of one of the colmatation parameters contradicts to the

others). Low level of correlation ($R^2 < 0.1$) or a mismatch in trend direction marked with gray color.

To estimate the influence of 13 parameters on colmatation process (feature importance arrangement) we should obtain single numerical criterion using R-squared statistics for all three parameters of colmatation equation 2. We used the following rule for averaging: $\overline{R^2} = 0.5\gamma(\overline{R_{TYPE II}^2} + \overline{R_{TYPE III}^2})$, where $\overline{R_{TYPE II}^2}, \overline{R_{TYPE III}^2}$ are means with respect to α, n , and R_{min} for each pressure drop Type. $\gamma = 0.66$ in case with mismatch in trend direction, and $\gamma = 1$ in case without mismatch.

Table 2. Analysis of rock properties influence on colmatation parameters.

Parameter	Type	R^2 for α	R^2 for n	R^2 for R_{min}	Parameter	Type	R^2 for α	R^2 for n	R^2 for R_{min}
K_{abs}	Type II	0.5	0.7	0.52	$d_g=0.1-0.25$ mm	Type II	0.42	0.52	0.29
	Type III	0.5	0.7	0.52		Type III	0.81	0.39	0.002
S_{or}	Type II	0.73	0.007	0.31	$d_g=0.05-0.01$ mm	Type II	0.56	0.49	0.36
	Type III	0.73	0.04	0.001		Type III	0.52	0.26	0.14
$d_p > 30\mu m$	Type II	0.6	0.8	0.48	quartz	Type II	0.28	0.02	0.78
	Type III	0.71	0.49	0.15		Type III	0.84	0.59	0.23
$d_p = 12-30\mu m$	Type II	0.55	0.015	0.11	microcline	Type II	0.21	0.02	0.71
	Type III	0.8	0.46	0.61		Type III	0.79	0.63	0.27
$d_p = 6-12\mu m$	Type II	0.73	0.29	0.25	dolomite	Type II	0.77	0.06	0.4
	Type III	0.91	0.35	0.27		Type III	0.49	0.03	0.05
$d_g = 0.25-0.5$ mm	Type II	0.62	0.67	0.24	anhydrite	Type II	0.7	0.68	0.27
	Type III	0.38	0.06	0.63		Type III	*	*	*

* not enough data for correlation

Bold underlined font stands for bad correlation (wrong trend or low R-squared).

Based on this analytical approach it was possible to investigate all the features of the self-colmatation process and arrange them in accordance with their importance (Figure 4). The absolute permeability and the fraction of pore throats with diameter larger than 30 μm had the strongest influence on colmatation. The smallest correlation was for the residual oil saturation and the fraction of grains with size 0.01-0.005 mm.

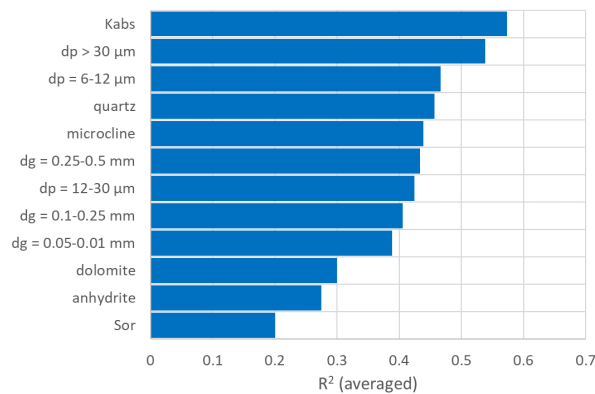


Figure 4. The factors affected on colmatation

drop and horizon types. Additional 3 features were Talakh, Khamakin and Botuobinsk horizons. The pressure drop was excluded from the features because it was a post experimental information (result of permeability depletion analysis).

Small dataset is a very essential problem to train and test the models. Another problem for machine learning algorithms is missing data in dataset: an ideal case is to

The second approach for investigating the influence of all the features on the self-colmatation have been dedicated to machine learning algorithms. The major benefit of this approach is a possibility to build complex prediction models of α, n , and R_{min} , where all features can be taken into account simultaneously.

For all predictive models we used 17 features: 14 features described earlier with the exception of pressure

have all features for each experiment. The grain size distribution, pore throat distribution and mineral composition analysis were performed not for all the core samples. Actual number of experiments with all 17 features was 5 tests out of 19. Thus, the first aim was to extract maximum information from our dataset.

To fill the missing data in dataset matrix we applied sequence of predictive procedures based on artificial neural network (ANN). Implementation of ANN has been done in Python environment. Python's scikit-learn library provides ANN representation in MLPRegression method [8]. The sequence of the procedures is the following. On first step we have predicted missing pore throat sizes distributions characteristics (for 6 tests) using a limited grain sizes distributions data (11 tests). On the second step an extended dataset (16 tests) have been used to predict all the missing grain sizes distributions characteristics (3 tests). And on the last step we have predicted characteristics of minerals distributions (for 9 tests) using all data recovered on previous steps. Completely recovered dataset matrix with 19 rows (tests) and 17 columns (features) was used then to build effective predictive models for α and n . And for R_{min} predictive we used model dataset matrix with 17 rows and 17 columns. Two experiments were excluded from the dataset in last case to obtain positive correlations in multivariable prediction.

We have considered 8 machine learning algorithms: 2 linear regressions with regularization (Lasso and Ridge); Decision Tree; Random Forest; Gradient Boosting; XG Boosting; SVR (implementation of Support Vector Machine method) and MLPRegressor (implementation of ANN) [9-13]. To evaluate the accuracy of the methods we have used the coefficient of determination R^2 . The same metrics has been used previously at independent feature analysis. To avoid overfitting of the model, there is a common practice to keep a part of the available data as a train and another part as a test set. The cross validation technique has been applied to estimate models' performance and compare them with each other. In Python's scikit-learn K-Folds cross-validator provides train/test indices to split data in train/test sets. K-Folds cross-validator splits dataset into k consecutive folds. Each fold is then used once as a validation while the $k - 1$ remaining folds form the training set. In all our cross-validations we used $k = 7$ data splits. It corresponds to 16 rows in training and 3 rows in testing.

The best result ($R^2 = 0.68$) for α model was obtained for XG Boosting algorithm. Performance of the model could be demonstrated by plotting predicted values versus observed values of porosity after ablation (Figure 5a). One can see that data points are located in a vicinity of the bisectrix.

The best result ($R^2 = 0.61$) for n model was obtained with Lasso algorithm (Figure 5b).

The best result ($R^2 = 0.44$) for R_{min} model was obtained with Gradient Boosting algorithm (Figure 5c).

To combine these three predictive models with formula (2) we can predict permeability reduction in time $K(t)/K_0$ using only 17 features of rock properties and flooding conditions for Vendian deposits. The major benefit of the intelligent analysis with machine learning algorithms is the dependence of colmatation parameters on all significant feathers simultaneously. It makes the machine learning models more robust than the 2D cross-plot correlations only. We can also show that for each α , n , R_{min}

coefficient of determination R^2 averaged for all features will be larger for the machine learning models than for manual analysis (Table 3). It is important to mention that relatively large R^2 in Table 3 could be explained by a relatively small initial dataset (with missing data). Even in this case intelligent analysis looks more precise than the manual method.

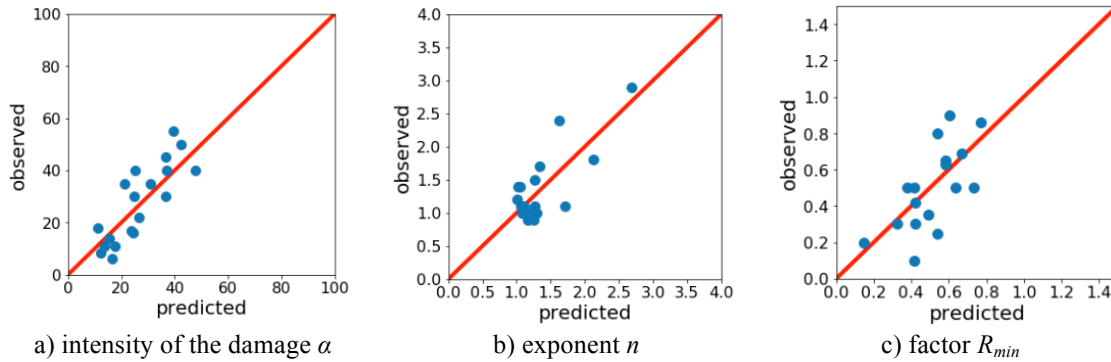


Figure 5. Comparison of real and predicted colmatation parameters.

Table 3. Models comparison

Colmatation coefficient	Averaged R^2 for all features (manual analysis)	R^2 (intelligent analysis)
α	0.62	0.68
n	0.36	0.61
R_{min}	0.33	0.44

Machine learning models also allow performing feature importance analysis directly without any assumptions and approximations. The Python's XGBoost method allows arranging features due to their influence on prediction model [11]. The XGBoost library provides a built-in function to plot features ordered by their importance and provides a score indicating how useful each feature was in the construction of the boosted decision trees within the model. The importance is calculated for a single decision tree by the amount that each feature split point improves the performance measure, weighted by the number of observations the node is responsible for. The feature importances are then averaged across all of the decision trees within the model. Results of feature importance analysis for α , n and R_{min} are presented in Figure 6.

Each colmatation parameter has its own most important feature: the content of microcline for α , the absolute permeability for n , and the fraction of pore throats with diameters 12-20 μm for R_{min} . We now consider the first five important features for α , n and R_{min} . We can see that 5 of 15 features could be found twice: the microcline content and the fraction of pore throats sizes $>30 \mu\text{m}$ (in Figure 6a and 6b); the absolute permeability and the fraction of pore throats sizes 6-12 μm (in Figure 6b and 6c); and the porosity (in Figure 6a and 6c). Accordingly, these five features have the dominant influence on the colmatation process.

It is also interesting to compare importance from intelligent and manual analysis. One can see that four of five features of dominant influence on the colmatation could be found within five most important features from Figure 4. This fact proves that both approaches do not contradict and demonstrate close results.

The example of prediction with both approaches is shown in Figure 7.

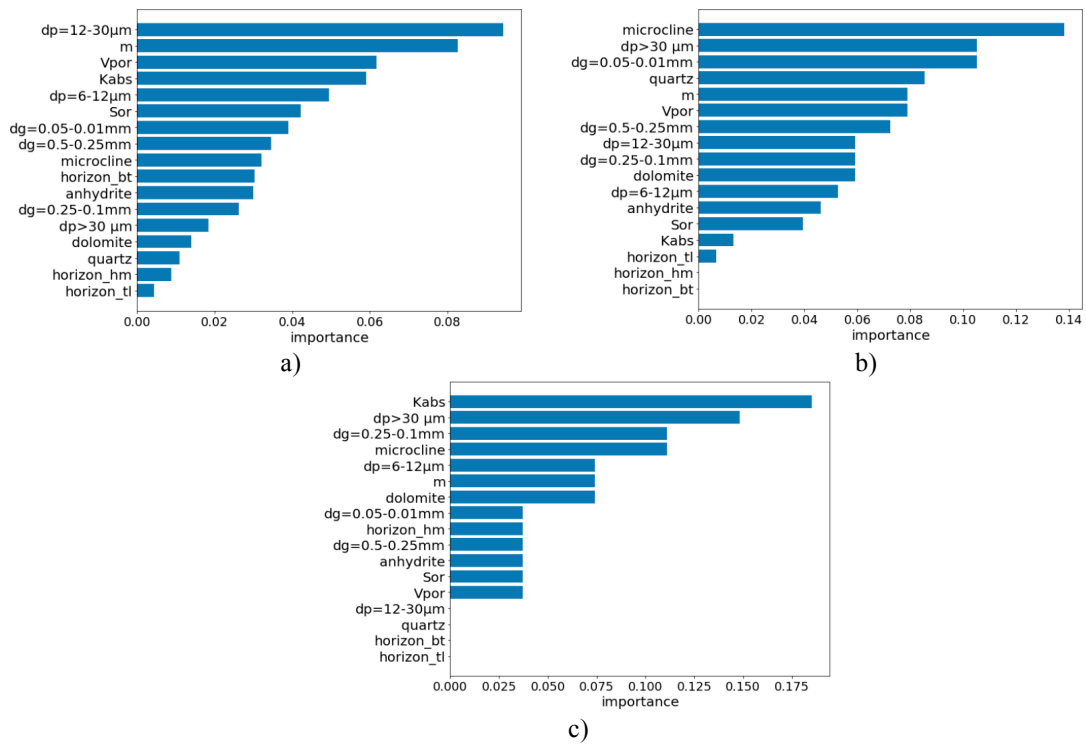


Figure 6. Results of feature importance analysis for α (a), n (b) and R_{min} (c).

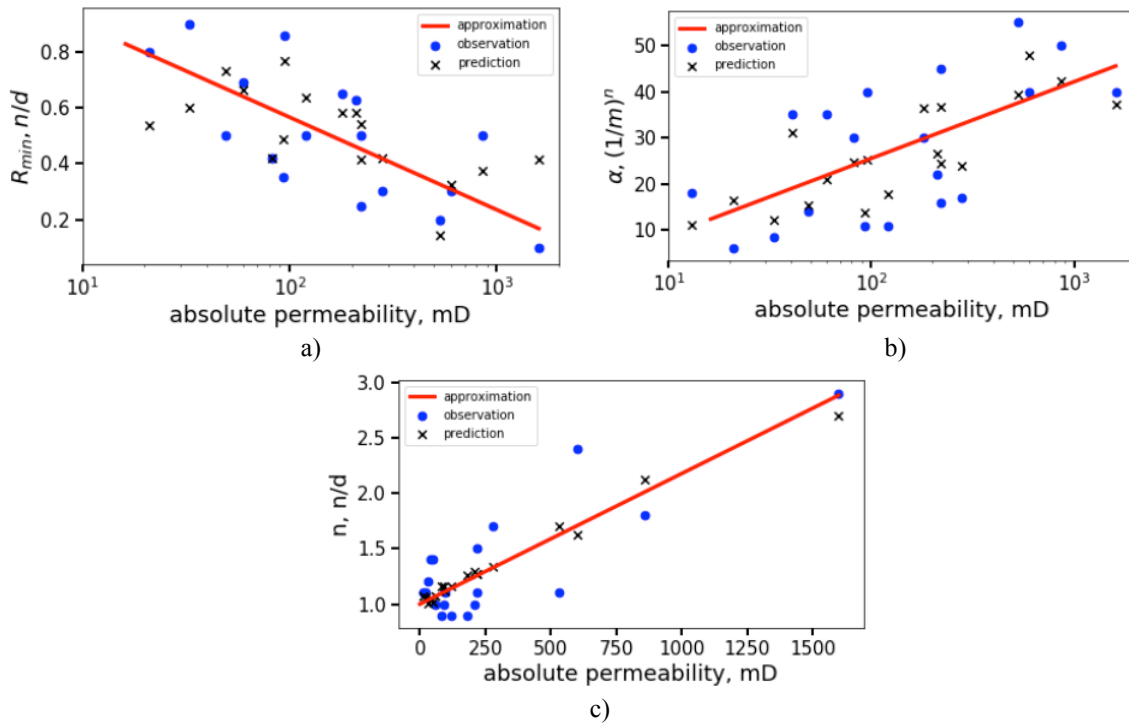


Figure 7. The example of prediction α (a), n (b) and R_{min} (c) prediction versus absolute permeability feature.

CONCLUSION

The predictive model of formation damage development in Vendian deposits based on the analysis of rock properties and flooding conditions has been developed. It is shown that machine learning algorithms allow to build precise prediction model of permeability reduction. All the features of the self-colmatation process have been arranged in accordance with their importance using two independent methods (cross-plot correlation estimations and joint XGBoost analysis). The most influencing features are permeability, porosity, fractions of pore throats with diameters 6-12 μm and $>30\mu\text{m}$ and content of microcline minerals in the rock.

REFERENCES

1. Civan F., *Reservoir formation damage*, Gulf Professional Publishing, (2015).
2. Boek E.S., Hall C., Tardy P.M.J., "Deep bed filtration modelling of formation damage due to particulate invasion from drilling fluids", *Transport in porous media*, (2012) **91**, 2, 479-508.
3. Orlov D., Koroteev D., Sitnikov A., "Self-Colmatation in terrigenous oil reservoirs of Eastern Siberia", *Journal of Petroleum Science and Engineering*, (2018) **163**, 576-589.
4. Lever A., Dawe R.A., "Water sensitivity and migration of fines in the Hopeman sandstone", *Journal of Petroleum Geology*, (1984) **7**, 1, 97-107.
5. Zeinijahromi A. et al., "Mathematical model for fines-migration-assisted waterflooding with induced formation damage", *SPE Journal*, (2013) **18**, 03, 518-533.
6. Gruesbeck C. et al., "Entrainment and deposition of fine particles in porous media", *Society of Petroleum Engineers Journal*, (1982) **22**, 6, 847-856.
7. Bachman R.C. et al., "Coupled simulation of reservoir flow, geomechanics, and formation plugging with application to high-rate produced water reinjection", *SPE Reservoir Simulation Symposium*, Society of Petroleum Engineers, 2003.
8. Pedregosa F. et al., "Scikit-learn: Machine learning in Python.", *Journal of machine learning research*, (2011) **12**, 2825-2830.
9. Boyd S., Vandenberghe L., *Convex optimization*, Cambridge university press, (2004).
10. Breiman L., "Random forests", *Machine learning*, (2001) **45**, 1, 5-32.
11. Friedman J.H., "Greedy function approximation: a gradient boosting machine", *Annals of statistics*, (2001), 1189-1232.
12. Cortes C., Vapnik V., "Support-vector networks", *Machine learning*, (1995) **20**, 3, 273-297.
13. Schmidhuber J., "Deep learning in neural networks: An overview", *Neural networks*, (2015) **61**, 85-117.